SPECTRAL STUDIES OF SHALLOW EARTHQUAKES AND EXPLOSIONS IN SOUTHERN CALIFORNIA

Peter M. Shearer and Bettina P. Allmann

University of California San Diego

Sponsored by Air Force Research Laboratory

Contract No. FA8718-06-C-0004

ABSTRACT

We compute and analyze *P*-wave spectra from over 300,000 earthquakes and 23,000 explosions recorded by over 300 seismic stations in southern California. We use an online waveform database stored on a RAID system at Caltech, which provides complete access to the Southern California Seismic Network (SCSN) seismogram archive. We compute spectra using a multi-taper method on 1.28 s noise and signal windows, positioned immediately before and after the *P* arrivals. After applying a signal-to-noise cutoff, we process the spectra using an iterative robust least-squares method to isolate source, receiver, and propagation path contributions. This corrects for first-order attenuation structure, as well as near-receiver site effects and any errors in the instrument response functions. Using the earthquake spectra and a simple source model, we compute an empirical Green's function to remove the tradeoff between the source terms and other terms in our model. Our observed earthquake spectra are fit reasonably well with a constant stress drop model over a wide range of moment. However, the explosion spectra show significant differences from the earthquake spectra, and often have a peak in their displacement spectra between about 3 and 8 Hz. Using this result, we develop and test a method to discriminate between shallow earthquakes and explosions using the relative amplitudes of the spectra within several different frequency bands. We compare results obtained for single explosions and ripple-fitted quarry blasts.

OBJECTIVES

The goal of this project is to systematically analyze and compare source spectra from over 340,000 earthquakes and explosions in southern California (Figure 1) to develop new insights into discrimination methods. Advances in data storage and computer capabilities make possible much more extensive analyses than have been performed in the past, which will provide a better picture of the distribution of source spectral properties and amplitudes. By examining tens of thousands of events, we will quantitatively characterize differences between earthquakes and explosions in terms of their spectral content and their P/S energy ratios. We also will identify and examine anomalous events, in particular earthquakes that may appear like explosions in spectral discrimination methods to determine how common they are and whether alternate discrimination techniques can be applied.

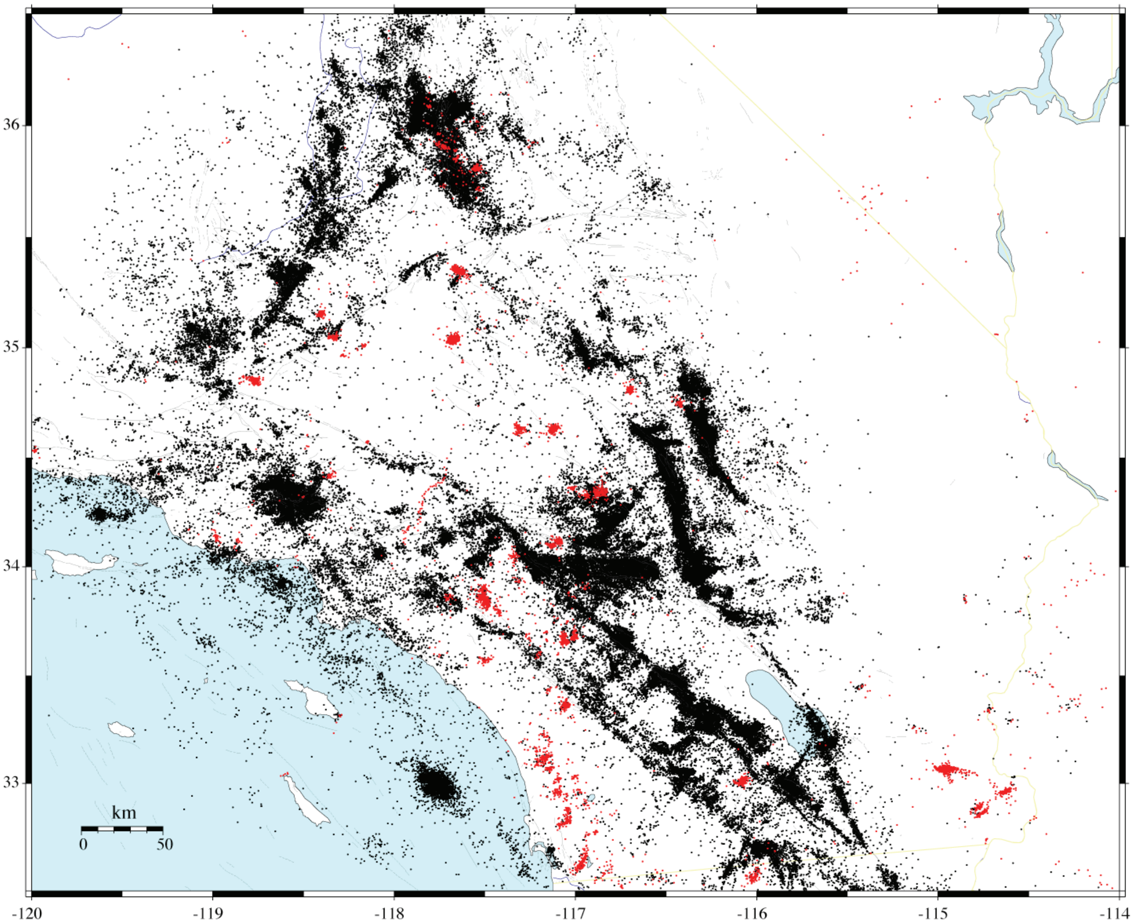

Figure 1. Locations of 319,750 earthquakes (black) and 23,748 explosions (red) in southern California from 1984 to 2002 as recorded by the SCSN. Figure adapted from Lin et al. (2006).

The project builds upon a recently completed large-scale analysis of southern California earthquake spectra (Shearer et al., 2006), to include a set of over 23,000 mining and other explosions between 1984 and 2004. The Shearer et al. earthquake study has already provided the largest set of earthquake spectra and stress drops computed to date, showing that individual event stress drops range between 0.2 and 20 MPa. The large number of stations and events available in southern California make possible empirical calibration methods to remove receiver response and path propagation effects. Our efforts focus on southern California because of the unmatched size and quality of the available data, but the results and insights will be applicable to other regions of more direct interest to nuclear monitoring programs.

In addition to computing and comparing stress drops between earthquakes and explosions, we will systematically analyze S-to-P amplitude ratios as a function of frequency and evaluate different discrimination strategies (e.g., Hedlin et al., 1990, 2004; Su et al., 1991; Walter et al., 1995; Stump et al., 2002; Leidig et al., 2004; Tibuleac et al., 2004). The large number of available events will make possible quantitative measures of the uncertainties in all of our computed parameters as well as missed and false detection rates in explosion discrimination methods.

RESEARCH ACCOMPLISHED

The SCSN has several hundred stations and records about 12,000 to 35,000 earthquakes each year. Recently, we began storing seismograms from all archived events in an online RAID system that provides rapid and random access to the data (Hauksson and Shearer, 2005). Spectra are computed as follows. For each seismogram, we pick the P and S arrivals. This is done using the operator pick, if available, or using the output of an automatic picking algorithm for a window around the predicted arrival time (based on the catalog event location and a 1-D velocity model). Traces are resampled to a uniform 100-Hz sample rate. Spectra are computed using a multitaper algorithm (e.g., Park et al., 1987) for 1.28 s noise and signal windows, immediately before and after the pick time. We compute results for all available channels and components for both P and S, including rotation of the horizontals (if present) into transverse and radial records. However, so far we have analyzed only P waves from the vertical EH (short-period) component. Both signal and pre-event noise spectra are corrected to displacement and stored in a special binary format. We note that these records generally clip for $M_L > 3.5$ earthquakes.

We apply a signal-to-noise (STN) cutoff to the spectra, requiring that the STN amplitude ratio be at least 5 for three separate bands of 5 to 10 Hz, 10 to 15 Hz, and 15 to 20 Hz. Next, we process the spectra to isolate source, receiver, and propagation path effects. This is an important step because individual spectra tend to be irregular in shape and difficult to fit robustly with theoretical models. However, by stacking and analyzing thousands of spectra, it is possible to obtain more consistent results. The basic approach is illustrated in Figure 2 and is similar to that used by Warren and Shearer (2000 and 2002) and Prieto et al. (2004). Each observed displacement spectrum $d_{ij}(f)$ from source i and receiver j is a product of a source term e_i (which includes the source spectrum and near-source attenuation), a near-receiver term s_j (which includes any uncorrected part of the instrument response, the site response, and the near-receiver attenuation), and a travel-time-dependent term $t_{k(i,j)}$ (which includes the effects of geometrical spreading and attenuation along the ray path). In the log domain, this product becomes a sum: $d_{ij} = e_i + s_j + t_{k(i,j)} + r_{ij}$ where r_{ij} is the residual for path ij. We parameterize t in terms of the predicted P travel time between the source and receiver, using the event locations and velocity model from Shearer et al. (2005). This accounts for both the event depth and the source receiver distance. The travel-time term $t_{k(i,j)}$ is discretized by its index k at 1 s increments in travel time. Because each station records multiple events and each event is recorded by multiple stations, this is an over-determined problem. We solve this equation using a robust, iterative, least-squares method in which we sequentially solve individually for the terms t_k, s_j, and e_i, keeping the other terms fixed at each stage. We suppress outliers by assigning L1-norm weights to misfit residuals greater than 0.2 s (or less than -0.2 s). This weighting scheme is necessary to ensure robustness with respect to a small number of spectra with large excursions compared to the bulk of the data. In practice, we found that the method converged rapidly to a stable solution after a few iterations.

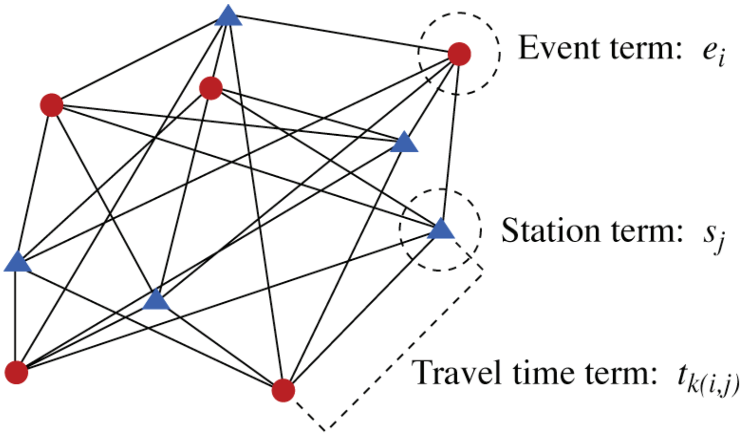

Figure 2. A cartoon showing how measured spectra can be modeled as a product of event, station, and travel-time-dependent terms.

Radiation pattern differences are not included in the previous equation and would be difficult to include in our processing because they are not generally available for the smaller-magnitude events. By using multiple stations for each source, however, radiation pattern effects will tend to average out. Note that this method resolves only differences in the relative shapes of the spectra. Without additional modeling assumptions, it cannot, for example, resolve how much of the spectral falloff is due to source effects and how much is due to attenuation common to all paths. The advantage of the method, however, is that it identifies and removes anomalies that are specific to certain sources or receivers. Because there may be difficulties in obtaining reliable and accurate instrument response functions for many of the stations in the archive, this is an important processing step that provides a way to correct for some of these problems.

Our focus has been on the stacked source spectra, e_i, which we ultimately use to estimate the moment and corner frequency of each event. At this stage, however, the source spectra only contain relative information among the different events. In order to estimate absolute spectra from our source stacks, we use the local magnitude M_L to obtain the scaling factor necessary to convert our relative moment estimates to absolute moment and we use an empirical Green's function approach to correct the spectral shapes for attenuation and other path effects (for details, see Shearer et al., 2006).

To study the average shape of the spectra, we stack our results within equally spaced bins in estimated seismic moment (obtained from the low-frequency part of the spectrum). Figure 3 shows these stacked spectra for both earthquakes and quarry blasts during 1994. The dashed lines show the best-fitting constant stress drop model of Madariaga (1976). One of the most active quarries is particularly anomalous and produces a bump in the spectra between about 3 and 8 Hz (seen in the middle panel of Figure 3). This bump largely disappears if this quarry is excluded from the analysis (see right panel of Figure 3).

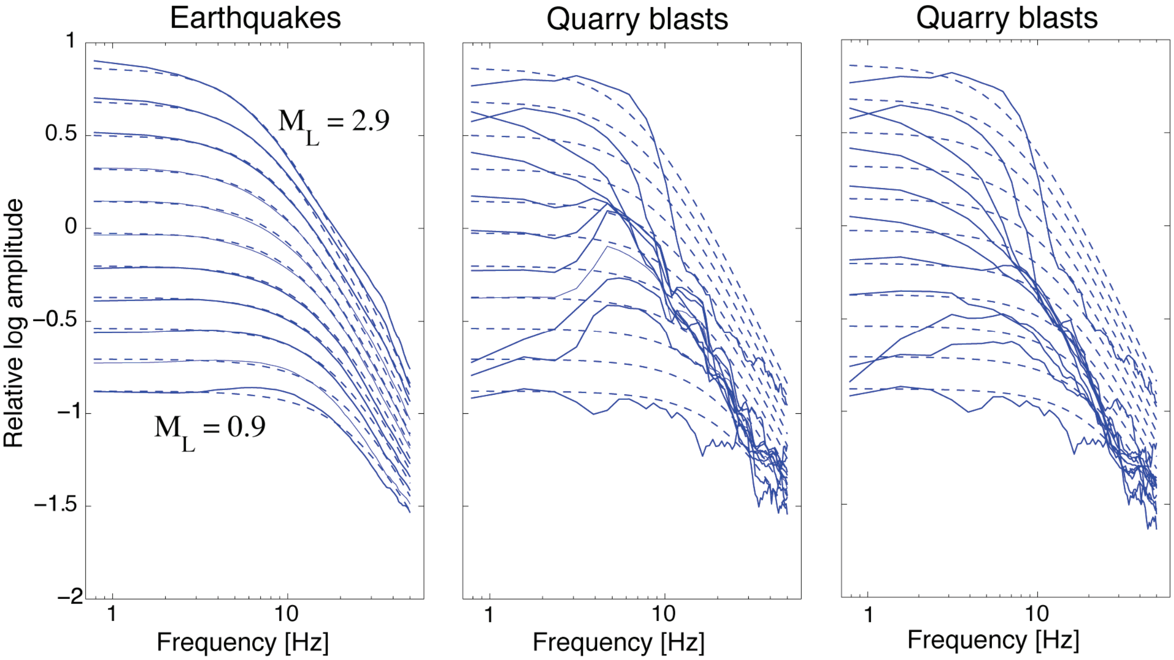

Figure 3. Stacked P-wave source displacement spectra from 1994 within bins of estimated seismic moment for: (left) 14,280 earthquakes, (middle) 360 quarry blasts, (right) 213 quarry blasts, excluding one particularly anomalous quarry. The spectra have been corrected for attenuation and other path effects using the empirical Green's function (EGF) method of Shearer et al., (2006). The dashed lines show the best-fitting constant stress drop model of Madariaga (1976).

Figure 3 shows that averaged earthquake spectra in southern California are well fit by a standard source model. However, the averaged quarry spectra appear anomalous in at least two respects: (1) they exhibit large misfit compared to the source model predictions, and (2) they have generally steeper falloffs at high frequencies than the model predictions, which will lead to lower corner frequencies and stress drop estimates. The lack of high-frequency radiation from the quarries is somewhat surprising and may reflect ripple firing and/or strong near-surface attenuation. In any case, we attempt to use these two differences to discriminate between earthquakes and quarry blasts in southern California.

Figure 4 plots root mean squared (RMS) misfit versus estimated stress drop for the Madariaga model. The quarry blasts have generally higher misfit and smaller estimated stress drops than the explosions. However, the two populations are not completely separated and there is a region of overlap. Figure 5 plots estimated moment versus corner frequency for the two sets of events. The quarry blasts exhibit a smaller range of moment and generally lower corner frequencies at the same moment, but again there is some overlap between the two groups.

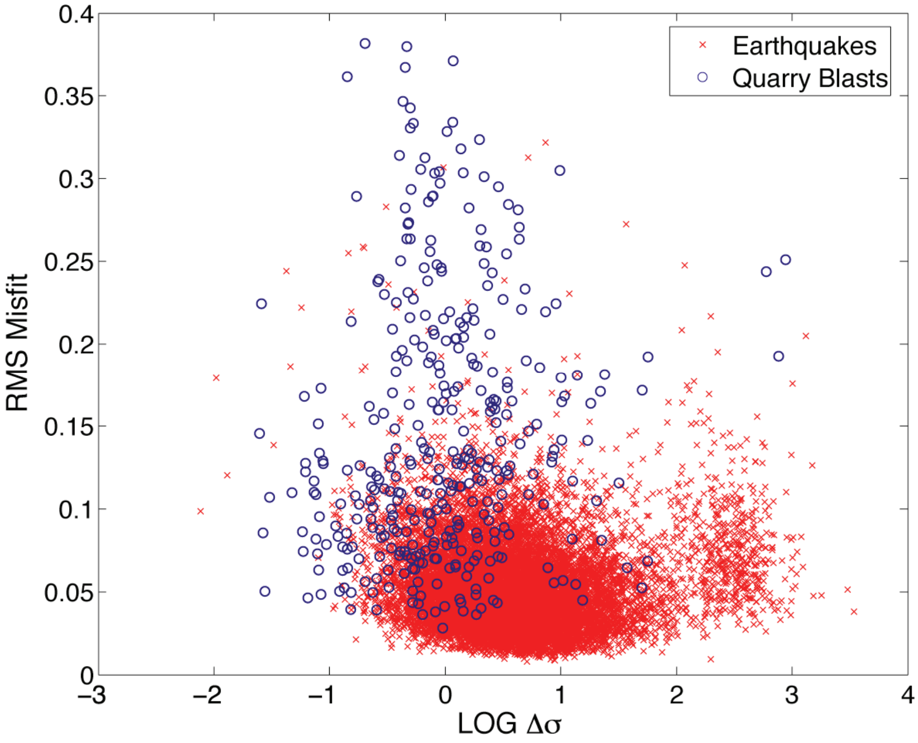

Figure 4. Spectral misfit to a standard source model versus estimated stress drop for southern California earthquake and quarry blasts during 1994. Earthquakes are shown in red, explosions in blue.

CONCLUSIONS AND RECOMMENDATIONS

Earthquakes and explosions in southern California exhibit significant differences in their average P-wave spectral properties. Quarry blast spectra are not well-fit by standard source models and typically have lower corner frequencies and anomalously steep falloffs at high frequencies compared to earthquakes of the same estimated moment. However, spectra from individual events have large variations and do not always permit an unambiguous identification of event type. Future results from analysis of S-wave spectra may provide additional discriminants.

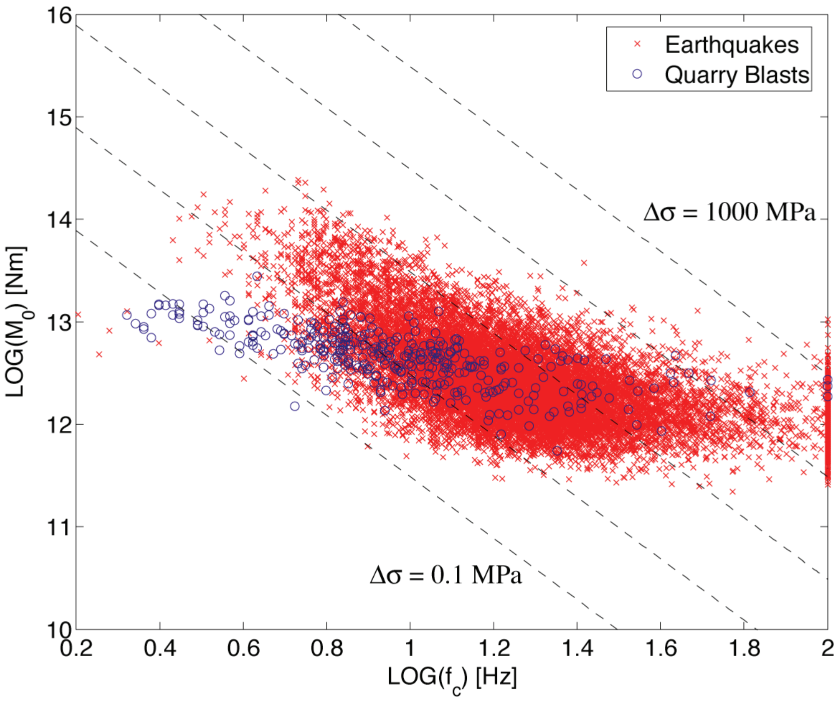

Figure 5. Moment versus observed corner frequency for southern California earthquakes and quarry blasts during 1994. The dashed lines show corresponding stress drop values from the Madariaga (1976) model. Earthquakes are shown in red and explosions in blue.

ACKNOWLEDGEMENTS

We thank Egill Hauksson for his help in maintaining the waveform database and computing the spectra and German Prieto for assistance in implementing the multi-taper algorithm.

REFERENCES

Hauksson, E. and P. Shearer (2005). Southern California hypocenter relocation with waveform cross-correlation, Part 1: Results using the double-difference method, *Bull. Seismol. Soc. Am.* 95: 896–903, doi:10.1785/0120040167.

Hedlin, M. A. H., J. -B. Minster, and J. A. O. Orcutt (1990). An automatic means to discriminate between earthquakes and quarry blasts, *Bull. Seismol. Soc. Am*. 80: pp. 2143–2160.

Hedlin, M. A., B. W. Stump, S. Arrowsmith, and M. D. Renwald (2004). A comparative test of seismic discriminants for mining explosions, in *Proceedings of the 26th Seismic Research Review*: *Trends in Nuclear Explosion Monitoring,* LA-UR-04-5801, Vol. 1, pp. 407–416.

Leidig, M. R., B. W. Stump, J. L. Bonner, C. T. Hayward, A. A. Velazco, D. F. Baker, H. Hooper, W. R. Walter, X. Yang, R. Zhou, C. L. Edwards, M. D. Renwald, and J. F. Lewkowicz (2004). Source phenomenology experiments in Arizona, in *Proceedings of the 26th Seismic Research Review: Trends in Nuclear Explosion Monitoring,* LA-UR-04-5801, Vol. 1 pp. 366–374.

Lin, G., P. Shearer, and Y. Fialko (2006). Obtaining absolute locations for quarry seismicity using remote sensing data. *Bull. Seismol. Soc. Am.* 96: pp. 722–728.

Madariaga, R. (1976). Dynamics of an expanding circular fault. *Bull. Seismol. Soc. Am*. 66: pp. 639–666.

Park, J., C. R. Lindberg, and F. L. Vernon, (1987). Multitaper spectral analysis of high frequency seismograms, *J. Geophys. Res*. 92: pp. 12,675–12,648.

Prieto, G. A., P. M. Shearer, F. L. Vernon, and D. Kilb (2004). Earthquake source scaling and self-similarity estimation from stacking P and S spectra, *J. Geophys. Res*. 109: doi:10.1029/2004JB003084.

Shearer, P., E. Hauksson, and G. Lin (2005). Southern California hypocenter relocation with waveform cross-correlation: Part 2. Results using source-specific station terms and cluster analysis, *Bull. Seismol. Soc. Am*. 95: pp. 904–915.

Shearer, P. M., G. Prieto, and E. Hauksson (2006). Comprehensive analysis of earthquake source spectra in southern California*, J. Geophys. Res*. 111: B06303, doi:10.1029/2005JB003979.

Stump, B., M. A. H. Hedlin, D. C. Pearson, and V. Hsu (2002). Characterization of mining explosions at regional distances, *Reviews of Geophysics*, 40: (4), 1011, doi:10.1029/1998RG000048.

Su, F., K. Aki, and N. N. Biswas (1991). Discriminating quarry blasts from earthquakes using coda waves, *Bull. Seismol. Soc. Am*. 81: pp. 162-178.

Tibuleac, I. M., J. Britton, D. B. Harris, T. Hauk, H. Hooper, and J. L. Bonner (2004). Detection methods for mining explosions in southern Asia, in *Proceedings of the 26th Seismic Research Review*: *Trends in Nuclear Explosion Monitoring,* LA-UR-04-5801, Vol. 1, pp. 427–438.

Walter, W. R., K. M. Mayeda, and H. J. Patton (1995). Phase and spectral ratio discrimination between NTS earthquakes and explosions, Part I: Empirical observations, *Bull. Seism. Soc. Am.* 85: pp. 1050–1067.

Warren, L. M. and P. M. Shearer (2000). Investigating the frequency dependance of mantle Q by stacking P and PP spectra, *J. Geophys. Res*. 105: 25, pp. 391–25, 402.

Warren, L. M. and P. M. Shearer (2002). Mapping lateral variations in upper mantle attenuation by stacking P and PP spectra, *J. Geophys. Res*. 107: pp. B12, 2342, doi:10.1029/2001JB001195.